

*Original Article*

## Electrical conductivity and physical changes of functionalized carbon nanotube/graphite/stainless steel (SS316L)/polypropylene composites immersed in an acidic solution

Hendra Suherman<sup>1\*</sup>, Abu Bakar Sulong<sup>2,3</sup>, Mohd Yusuf Zakaria<sup>2</sup>,  
Nishata Royan<sup>2,3</sup>, and Jaafar Sahari<sup>2,3</sup>

<sup>1</sup> Department of Mechanical Engineering, Universitas Bung Hatta, Padang, West Sumatra, 25143 Indonesia

<sup>2</sup> Fuel Cell Institute, Universiti Kebangsaan Malaysia, Selangor, 43600 Malaysia

<sup>3</sup> Department of Mechanical and Material Engineering, Universiti Kebangsaan Malaysia, Selangor, 43600 Malaysia

Received: 22 June 2016; Revised: 18 September 2016; Accepted: 1 November 2016

---

### Abstract

Chemical functionalization of carbon nanotubes (CNTs) and graphite (G) was performed to improve their adhesion to a metal powder (SS316L) and a polypropylene (PP) matrix. A conductive pathway was thus formed to utilize the high electrical conductivity of the SS316L for conductive polymer composites (CPCs) applications. The rheological properties of the feedstock mixture were measured, and samples were formed by injection molding. Fourier transform infrared spectroscopy indicated the existence of functional groups generated by chemical wet oxidation. Only feedstock mixtures containing more than 28 vol% of the PP composite showed a shear rate ( $10^2 \text{ s}^{-1}$  to  $10^5 \text{ s}^{-1}$ ), shear viscosity ( $10 \text{ Pa}\cdot\text{s}$  to  $10^3 \text{ Pa}\cdot\text{s}$ ), and flow behavior index ( $n < 1$ ) suitable for injection molding. The functionalized composites exhibited improved electrical and mechanical properties over the as-produced composites. The functionalized composites containing 28 vol% PP obtained an electrical conductivity of 6 S/m, compared to 0.5 S/m for the as-produced composites.

**Keywords:** conductive polymer composites (CPCs), carbon nanotubes (CNTs), stainless steel powder, electrical conductivity, corrosion

---

### 1. Introduction

Conductive polymer composites (CPCs) are materials formed from a mixture of a conductive filler, such as carbon nanotubes (CNTs), carbon black (CB), carbon fiber (CF), or conductive polymers, and a conventional polymeric binder (Castro *et al.*, 2011; Chunhui *et al.*, 2008). CPCs are advantageous in many applications because of their low cost,

light weight, and good corrosion resistance (Bin *et al.*, 2006). These properties are advantageous for the production of CPCs with a well-balanced performance-to-price ratio. Theoretically, a polymer matrix is an insulator by nature; when a certain amount of filler is added to the mixture (reaching a critical content) the electrical behavior of the polymer matrix becomes conductive (Antar *et al.*, 2012).

A cost-effective processing method capable of producing CPCs on a large scale is necessary due to the increasing demand for CPCs. Injection molding is a promising candidate; it is suitable for mass production, carries a low production cost, and can produce complex parts that are close to the final required shape (Stobinski *et al.*, 2010). To achieve higher electrical conductivity, the conductive filler loading

---

\*Corresponding author

Email address: henmeubh@yahoo.com;  
hendras@bunghatta.ac.id

must be increased, which increases the viscosity of the CPCs accordingly. The material's viscosity is a critical processing factor that allows the composite melt to fill the cavity of the mold before solidifying; a high feedstock viscosity makes the injection molding process difficult (Cao *et al.*, 1991). Injection molding requires specific rheological properties, such as a flow behavior index of  $n < 1$ , indicative of pseudoplastic behavior, and a moderate activation energy  $E_a$ , which serves as a measure of the sensitivity of the flow to temperature changes (Yang *et al.*, 2003).

CNTs are well-known conductive fillers that improve the electrical, mechanical, morphological, and thermal properties of polymer composites. CNTs possess a large aspect ratio, excellent conductivity, and a low percolation threshold (Imai *et al.*, 2010; Zhang *et al.*, 2009), but these properties are often not fully utilized when CNTs are combined with a polymer matrix in composites (Sharma *et al.*, 2009). The reasons for this inefficiency are the poor surface interaction between CNTs and polymeric materials and the entangled nature of CNTs, which leads to poor dispersion into the polymer matrix.

Chemical functionalization of CNTs provides a better interaction with the polymer matrix than physical functionalization does, although excessive chemical functionalization may damage the CNTs (Ma *et al.*, 2010). The electrical conductivity of CPCs relies on the uniform dispersion of the electrically conductive fillers to form a more continuous electron pathway throughout the insulating binder (Bodo *et al.*, 2006). Chemical modification of the surface of the carbon fillers is often performed to contribute to the uniform spread of the material and to enhance the adhesion by building functional groups that relieve the hydrophobicity and inert properties in order to increase the electrical conductivity of the CPCs (Chang *et al.*, 2009; Nishata *et al.*, 2013).

Corrosion may occur in the metallic fillers within the composite, and dissolution is a possibility when the metals are operating in an acidic environment (pH 2 to pH 4) at a temperature of approximately 80 °C (Antunes *et al.*, 2010). For these reasons, the objectives of this study are to investigate both the flow ability of the feedstock for novel CNT/G/SS316L/PP composites and the effect of a corrosive environment on the electrical and mechanical properties of functionalized and as-produced CNTs/G/SS316L/PP composites.

## 2. Experimental

### 2.1 Polymer matrix and conductive fillers

The PP polymer matrix (pellet form) was obtained from Polypropylene Malaysia with a density of 0.91 g/cm<sup>3</sup> and a melting point of 160 °C. Our group has studied different types of polymer matrices such as Epoxy (EP) for thermoset (Suherman *et al.*, 2013) and PP for thermoplastic (Dweiri *et al.*, 2007; Selamat *et al.*, 2011). Many researchers also choose PP as a polymer matrix and mix different types of fillers (Lee *et al.*, 2011; Liao *et al.*, 2008). PP was used as a polymer matrix and reinforcement fillers were natural graphite 3243 purchased from Asbury Carbons with a size of 30 µm, a surface area of 3.0 m<sup>2</sup>/g, and a density of 0.47 g/cm<sup>3</sup>. Our previous results showed that natural graphite polymer composites boost the electrical conductivity by more than

100% compared to synthetic graphite polymer composites (Dweiri *et al.*, 2007; Suherman *et al.*, 2010). Therefore, natural graphite was chosen as the primary filler in this study. The multi-walled CNTs were obtained from Nanocyl Belgium with a density of 0.065 g/cm<sup>3</sup> and a particle size of 9.5 nm in diameter and 1.5 µm in length. Water-atomized stainless steel SS316L with an average particle size of 50 µm and a density of 2.7 g/cm<sup>3</sup> was purchased from Epson Atmix Corporation. The G and CNTs were functionalized via wet oxidation by immersing the materials in the oxidizing agent and stirring using a magnetic stirrer for 48 hours at 200 rpm at 180 °C. The solution was then neutralized to pH 7, filtered, and the material was dried at 40 °C for 24 hours. The presence of functional groups on the G and CNTs was verified through FTIR spectroscopy.

### 2.2 CPC fabrication and characterization

The functionalized CNTs are expected to disperse throughout the polymer matrix. A small amount of pristine CNTs as conductive fillers were already successfully produced using EP as a matrix (Suherman *et al.*, 2010; Suherman *et al.*, 2013). Carbon black as a conductive filler with PP has also been used to produce CPCs (Dweiri *et al.*, 2007; Selamat *et al.*, 2011).

The conductive fillers were mixed into the polymer matrix with a Brabender twin screw extruder at 180 °C and a rotational speed of 50 rpm for 20 minutes. The mixed feedstock was then crushed into granules. The characterization of the rheological properties was carried out with a Shimadzu CFT-500D rheometer to determine whether the flow characteristics of the feedstock would be suitable for the injection molding process (Ibrahim *et al.*, 2011). The specimen was formed by a 100 cc plunger-type micro injection molding with the following parameters: mold temperature (70°C), packing pressure (5 sec), injection pressure (10 bar), and injection temperature (200 °C) (Ibrahim *et al.*, 2009). The in-plane electrical conductivity of the CPCs was measured using a four-point probe (Jandel RM3-AR) (Suherman *et al.*, 2010). The corrosion resistance was determined by immersing the samples into 0.5 M sulfuric acid and then measuring the weight loss with a mass balance (accurate to 0.0001 g) every third day for 12 days (288 hours). The potentiodynamic and potentiostatic are the proper tests to measure the corrosion rate. In this study, we focus on the observed physical changes caused by immersion in acidic solution. Similar methods have been previously reported in the literature (Paul *et al.*, 2012). The fractured surfaces from the flexural test were observed with a Hitachi S-4700 scanning electron microscope (SEM). The flexural test was conducted using an INSTRON 5567 according to ASTM D790.

## 3. Results and Discussion

### 3.1 Functionalization of CNTs and G

Figure 1a shows the FTIR spectra for the as-produced and functionalized CNTs. The spectra contain intense bands at 3,500 cm<sup>-1</sup> to 3,250 cm<sup>-1</sup>, 2,500 cm<sup>-1</sup> to 2,000 cm<sup>-1</sup>, 1,750 cm<sup>-1</sup> to 1,500 cm<sup>-1</sup>, and 1,250 cm<sup>-1</sup> to 1,000 cm<sup>-1</sup>, indicative of -OH, -N=C=O, and C=O bond formation, along

with O-H and C-O deformation on the surface of the CNTs (Stobinski *et al.*, 2010). Figure 1.b shows the FTIR spectra of the as-produced and functionalized G; the bands at  $2,500\text{ cm}^{-1}$  to  $1,750\text{ cm}^{-1}$  indicate the introduction of C=O and -N=C=O to the G surface. These functional groups serve to adjust the hydrophobic and inert characteristics of the CNTs and G surfaces, reducing the difference in surface energy between the polymer matrix and the carbon surface and enhancing the wetting of the polymer on the CNTs and G. These polymer/filler interactions play an important role in the electrical and mechanical properties of the resulting CPCs.

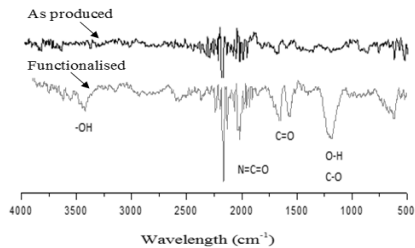


Figure 1a. FTIR spectra of the as-produced and functionalized CNTs.

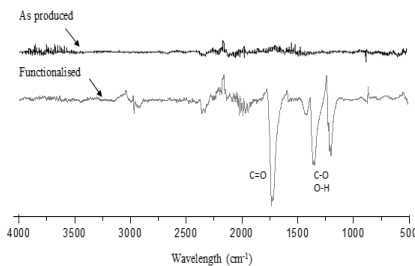


Figure 1b. FTIR spectra of the as-produced and functionalized graphite.

### 3.2 Rheological properties

Figure 2 shows the variation of the viscosity with shear rate at various temperatures for different matrix compositions in vol% PP. The composition of (25, 28, 30, 35, and 30/70 vol. % PP) show the same trend, where the increase shear rate will reduce the viscosity of CPCs, with the maximum value of share rate around  $4\text{ s}^{-1}$  at temperature of  $200\text{ }^{\circ}\text{C}$ . On composition of 25 vol. % PP (Figure 2a) seen that the viscosity of CPCs decrease from  $3.7\text{ Pa}\cdot\text{s}$  to  $3.3\text{ Pa}\cdot\text{s}$  at temperature of  $180\text{ }^{\circ}\text{C}$  with the increasing of shear rate from  $1.1\text{ s}^{-1}$  to  $2\text{ s}^{-1}$ . Furthermore at temperature of  $190\text{ }^{\circ}\text{C}$  the viscosity of CPCs decrease from  $3.65\text{ Pa}\cdot\text{s}$  to  $3\text{ Pa}\cdot\text{s}$  at  $2.4\text{ s}^{-1}$  shear rate, and viscosity of CPCs decrease from  $3.6\text{ Pa}\cdot\text{s}$  to  $2.55\text{ Pa}\cdot\text{s}$  at  $2.8\text{ s}^{-1}$  shear rate value on temperature of  $200\text{ }^{\circ}\text{C}$ . All of the composites exhibit pseudoplastic behavior, in which the viscosity of the CPCs decreases with increasing shear rate.

Figure 3 also indicates that the viscosity and shear rate values are in the acceptable range for injection molding ( $10\text{ Pa}\cdot\text{s}$  to  $1,000\text{ Pa}\cdot\text{s}$  and  $10^2\text{ s}^{-1}$  to  $10^5\text{ s}^{-1}$ , respectively). Except for CPCs with 25 vol% PP, the feedstock viscosities all exceed  $1,000\text{ Pa}\cdot\text{s}$ ; as a result, only the 25 vol% PP feedstock is suitable for injection molding at low temperature and low injection pressure (Ibrahim *et al.*, 2011; Yimin *et al.*, 2007). Figure 3 shows the variation of the viscosity with temperature at various shear rates for different matrix compositions.

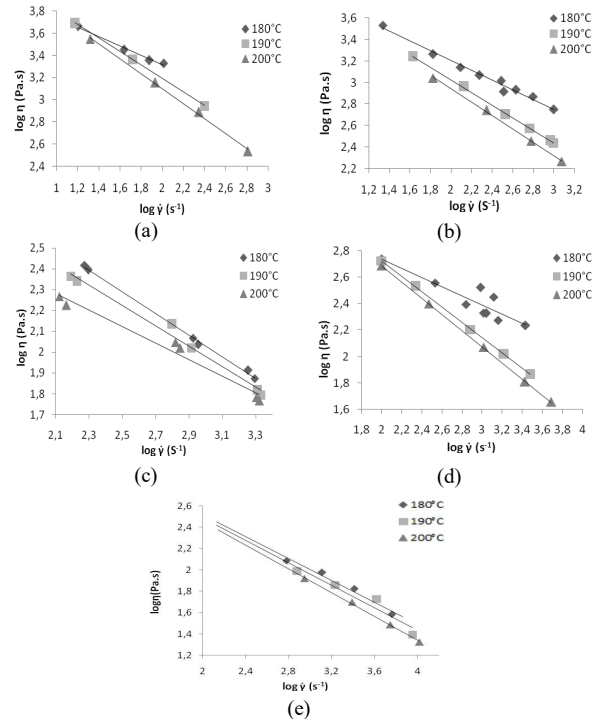


Figure 2. Variation of the viscosity with shear rate at various temperatures for different matrix compositions (vol% PP) (a) 25, (b) 28, (c) 30, (d) 35, and (e) 30/70 SS316L (reference).

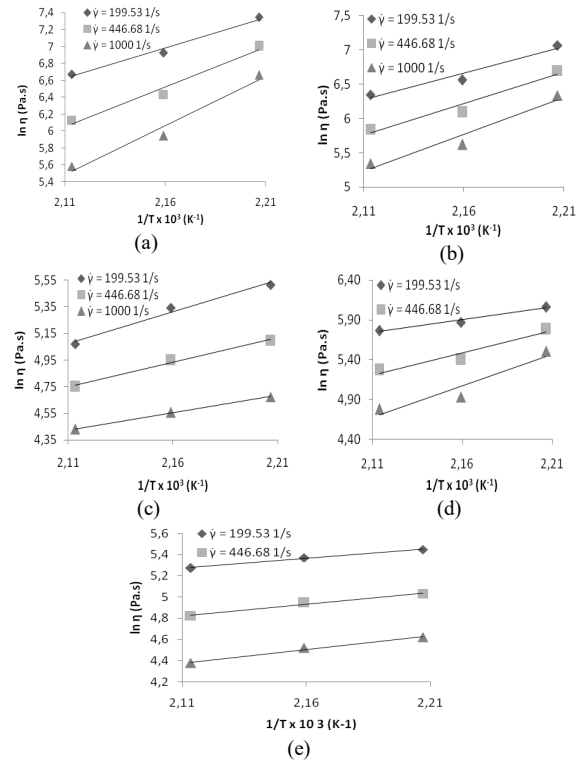


Figure 3. Variation of the viscosity with temperature at various shear rates for different matrix compositions (vol% PP) (a) 25, (b) 28, (c) 30, (d) 35, and (e) 30/70 SS316L (reference).

Table 1 summarizes the variation of the activation energy and the flow behavior index of the CNT/G/SS316L/PP composites of various compositions at a shear rate of  $1,000 \text{ s}^{-1}$ . All of the CPCs have a higher activation energy ( $E_a$ ) than the reference composite (PP/SS316L at 30/70 vol%), indicating a greater sensitivity of the composite's rheological properties to temperature changes (Bodo *et al.*, 2006; Chen *et al.*, 2008). Evidently, the rheological behavior of the composites is affected by the type, size, and shape of the fillers.

Table 1. Change in the activation energy, flow behavior index, and mold ability index of CNT/G/SS316L/PP composites shear rate of  $1000 \text{ s}^{-1}$ .

| Feedstock                              | Activation energy, $E_a$ (kJ/mol) | Reference viscosity $\eta_0$ (Pa.s) | Temperature ( $^{\circ}\text{C}$ ) | Flow behavior index, $n$ |
|--|-----------------------------------|-------------------------------------|------------------------------------|--------------------------|
| 25% PP                                 | 96.16                             | 6.09E-09                            | 180                                | 0.6555                   |
|  |                                   |                                     | 190                                | 0.5766                   |
|  |                                   |                                     | 200                                | 0.4821                   |
| 28%PP                                  | 88.69                             | 3.16E-08                            | 180                                | 0.5475                   |
|  |                                   |                                     | 190                                | 0.4151                   |
|  |                                   |                                     | 200                                | 0.3783                   |
| 30%PP                                  | 21.71                             | 3.38E-1                             | 180                                | 0.4783                   |
|  |                                   |                                     | 190                                | 0.4025                   |
|  |                                   |                                     | 200                                | 0.3611                   |
| 35%PP                                  | 65.15                             | 7.12E-06                            | 180                                | 0.4323                   |
|  |                                   |                                     | 190                                | 0.3789                   |
|  |                                   |                                     | 200                                | 0.3475                   |
| 30%PP/<br>70%SS316<br>L<br>(reference) | 21.52                             | 3.40E-1                             | 180                                | 0.486                    |
|  |                                   |                                     | 190                                | 0.473                    |
|  |                                   |                                     | 200                                | 0.444                    |

### 3.3 Electrical conductivity of the CPCs before and after the corrosion test

Figure 4a and b shows the electrical conductivity of the as-produced and functionalized composites before and after corrosion testing by immersion in acidic solution. The electrical conductivity of both types of CPCs decreases with increasing PP content. Moreover, the composites containing functionalized CNTs and graphite have higher electrical conductivity (6 S/m) than the as-produced composites (0.5 S/m). These results agree with those published by Liao *et al.* (2008), who found that functionalizing CNTs causes an increase in the continuity of the electron flow by allowing a more uniform dispersion throughout the composite mixture.

Larger sized graphite reduces the contact resistance between the filler particles, while smaller-sized CNT fillers contribute to a greater increase in the conduction path; both of

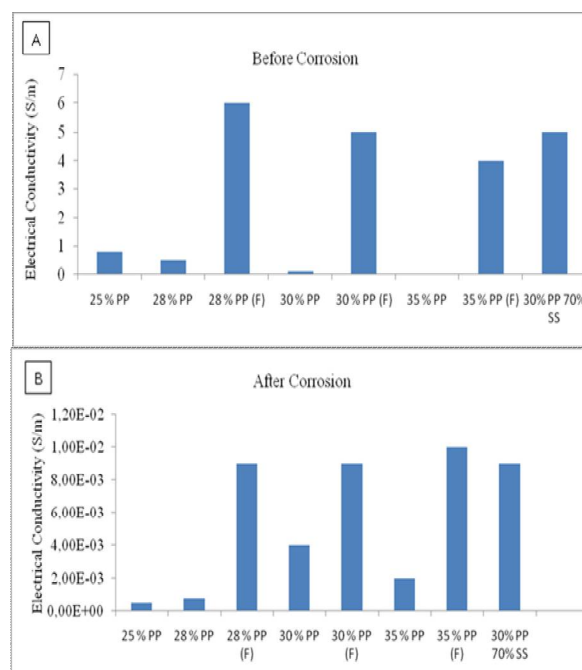


Figure 4. Electrical conductivity of the as-produced and functionalized composites before (5a) and after corrosion (5b) by immersion in acidic solution

these effects improve the electrical conductivity of the composite. The functionalized fillers also increase the adhesion capability of the other materials in the CPCs (SS316L and PP), provide more surface contact, and contribute to a higher conductivity (Liao *et al.*, 2008). As-produced CNTs tend to self-agglomerate, which causes reduced electrical conductivity. However, excessive modification of CNTs can lead to defects in their structure. The theoretical conduction mechanism between the CNTs, graphite, and SS316L powders within the PP polymer matrix is illustrated in Figure 5.

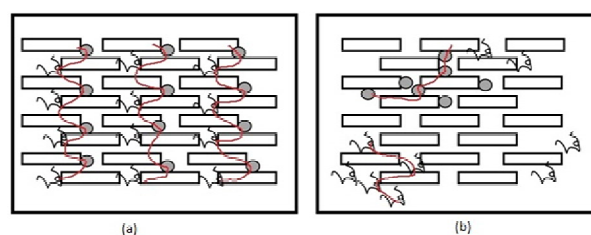


Figure 5. Conductive mechanism in a CPC plate with: (a) functionalized CNTs distributed homogeneously and (b) as-produced CNTs. Graphite (rectangular), CNT (black curl) and SS316L (circle) forming conductive paths (line).

This behavior is related to percolation theory, wherein the maximum electrical conductivity is achieved when the conductive filler content of the composite surpasses the percolation threshold. Therefore, a decrease in conductive fillers causes a decrease in the composite's electrical conductivity. Moreover, an increase in the PP content leads to increases in the size of regions that separate the conductive

filler particles, thus disturbing the electron flow and reducing the electrical conductivity (Antunes *et al.*, 2011).

Our previous work in compression molded thermo-plastic PP (Dweiri & Sahari, 2007; Selamat *et al.*, 2011) and thermoset EP (Suherman *et al.*, 2010; Suherman *et al.*, 2013) showed that compression molded plates are able to meet the DOE target of an in plane conductivity higher than 100 S/cm (Suherman *et al.*, 2013). However, this research results using injection molding show that the electrical conductivity is very low, which is only 0.06 S/cm. Our theoretical explanation of the lower electrical conductivity is that not all of the fillers which are fed into the hopper are able to go through the barrel and fill the cavity. Thus, there is less filler in the injection molded plates, which is expected to lead to significantly reduced electrical conductivity. Our group has also studied the effect of carbon black (CB) and CNTs as secondary fillers with G as the primary filler (Dweiri & Sahari, 2007; Suherman *et al.*, 2010; Suherman *et al.*, 2013). We found that CNTs/G composites have better electrical properties compared to CB/G composites. The electrical conductivity is increase by more than 200%. The method of dispersion of the CNTs and G through an internal mixer (mechanical mixer) has been used in previous studies for the preparation of feeds tocks for compression molding (Suherman *et al.*, 2010; Suherman *et al.*, 2013). The resulting composites show an electrical conductivity greater than 100 S/cm, which meets DOE requirements. Therefore, we chose CNTs as secondary filler. The amount of fillers (CNTs and G) in the polymer matrix is limited based on the rheological properties, as presented in Figure 2 and 3, and Table 1. The compositions used in this study have a viscosity less than 100 Pa·s, a shear rate between  $10^2 \text{ s}^{-1}$  and  $10^3 \text{ s}^{-1}$  and a flow ability index below 1. These criteria must be met by the feedstock to ensure that it fills the cavity (German & Bose, 1997; Rosato & Rosato, 1995).

Figure 6 shows the weight loss of the CPCs (%) after the corrosion test (immersion in acidic solution). All samples were immersed in a corrosive 0.5 M sulfuric acid aqueous solution and lost mass during the immersion period due to pitting, which involves the release of metal cations and flaking of the formed oxide, which does not firmly adhere to the metal surface (Kadry, 2008; Paul *et al.*, 2012).

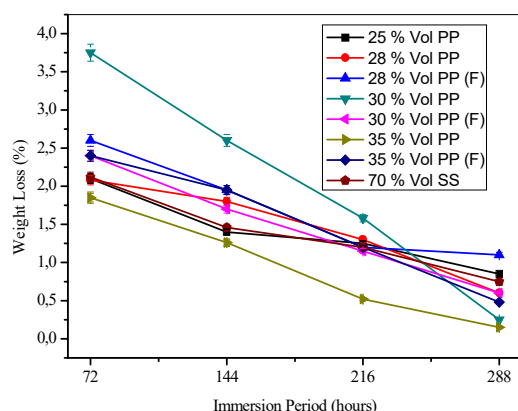


Figure 6. Weight loss of CPC (%) after corrosion testing by immersion in acidic solution.

The results shown in Figure 6 indicate that the weight percentage loss decreases with increasing immersion time; this decrease is due to the formation of an oxide layer, which attains significant thickness and forms a passivated layer that protects against the corrosive environment (Paul *et al.*, 2012; Stobinski *et al.*, 2010). However, this oxide layer causes a decrease in the current density; because the electrical conductivity is proportional to the current density, the electrical conductivity of the composite also drops, as shown in Figure 4a and b.

Figure 7 shows SEM images of the fractured surface of as-produced and functionalized CNT/G/SS316L/PP composites. The functionalized CNTs (Figure 7b) shows better disperse of CNTs and less voids within polymer matrix compare to the as-produce CNTs (Figure 7a), thus create more conductive network between the graphite, the SS316L powder, and resulting a better electrical conductivity.

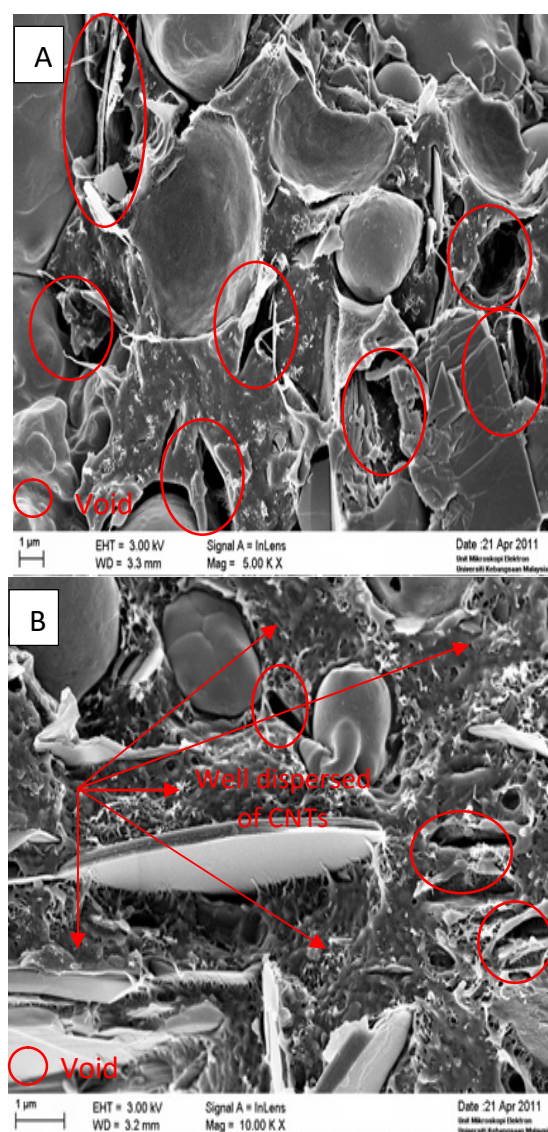


Figure 7. Fracture surface SEM images of the CNTs/G/SS316L/PP composites (a) as-produced and (b) functionalized condition.

Figure 8 shows the SEM images of SS316L powder embedded in the CPC matrix both before and after the corrosion test. Pitting is observed on the SS316L powder component of the 28 vol% PP composite exposed to the corrosive environment, as is evident in Figure 8(b). The pitting occurs on the composite because the acidic conditions induce the formation of a localized hole on the surface by anodic and cathodic reactions, which creates the tendency of a negative ion to migrate into the existing hole, causing the hole to grow further. The effect of this type of corrosion on the weight reduction of the composite is relatively small; however, after a longer period of time, pitting can lead to structural damage.

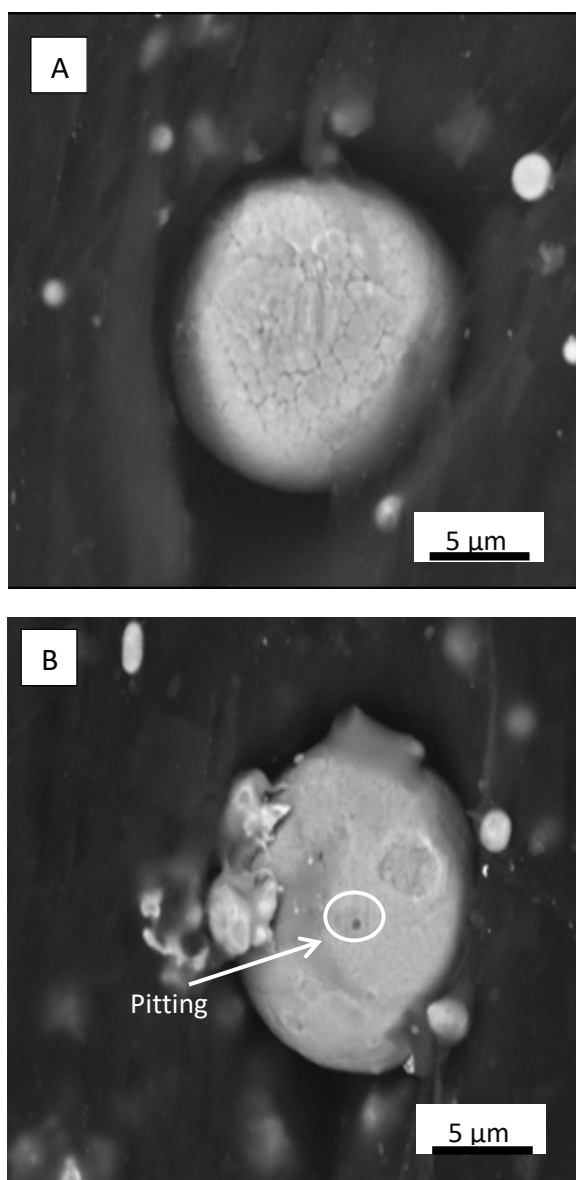


Figure 8. SEM image of SS316L powder on CPCs (a) before and (b) after corrosion.

### 3.4 Mechanical properties

Table 2 shows the flexural properties (flexural strength, flexural modulus, and elongation) of the different CNT/G/SS316L/PP composites. First, the flexural strength and elongation increase with increasing PP content; this increase occurs due to better wetting at higher PP loading, which leads to an increase in the amount of polymer coating the filler surface (Dweiri & Sahari, 2007).

Table 2. Flexural properties variation of the CNT/G/SS 316L/PP composites.

| Sample  | Flexural Strength (MPa) | Flexural Modulus (MPa) | Elongation (mm) | Maximum load (N) |
|---------|-------------------------|------------------------|-----------------|------------------|
| AP 28   | 73.443±2.6              | 10550±1607             | 1.837±0.2       | 22.702±0.8       |
| AP 30   | 74.495±2.9              | 10083±869              | 1.845±0.1       | 23.027±0.9       |
| AP 35   | 81.019±0.2              | 9333±144               | 3.206±0.3       | 25.044±0.1       |
| F 28    | 77.142±2.7              | 10861±427              | 0.484±0.8       | 24.155±0.8       |
| F 30    | 78.046±1.1              | 9972±708               | 3.794±0.1       | 23.816±0.3       |
| F 35    | 83.917±4.5              | 9100±259               | 6.634±1.2       | 25.940±1.4       |
| AP30/70 | 43.961±2.0              | 11105±764              | 9.514±0.1       | 13.589±0.6       |

In addition, the functionalized CNT/G/SS316L/PP composites have better flexural strength and elongation than the as-produced CNT/G/SS316L/PP composites. The flexural strength increases from 81 MPa to 84 MPa and the elongation increases from 3 mm to 6 mm with the inclusion of the functionalized CNTs at 35 vol% PP. This behavior is similar to that of the electrical conductivity of the functionalized composite because the electrically conductive networks, as shown in Figure 5a, also acts as reinforcement for the enhancement of load transfer during flexural testing. The load is absorbed by the CNTs and G first before being distributed to the polymer matrix. Conversely, the flexural modulus of the CPCs decreases with increasing PP content. The reference CPC, containing 30 vol% PP and 70 vol% SS316L, provides the lowest flexural strength, displaying a brittle behavior. Based on the properties, functionalized composites containing 28 vol % PP can be used as electrical devices.

### 4. Conclusions

Functionalized CNT/G/SS316L/PP composites exhibited improved electrical and mechanical properties compared with as-produced CNT/G/SS316L/PP composites. The improved behavior of the functionalized composites was due to the formation of an electrically conductive pathway and reinforced network, which led to more effective electron and load transfer. The rheological characterization of the feedstocks showed that PP content above 28 vol% was necessary for producing composites by the injection molding process. All composites showed decreased electrical conductivity after immersion in an acidic solution; higher concentrations of SS316L metal powder in the composites caused a greater decrease. Further investigation of the improvement of the electrical conductivity should be carried out in the future.

## Acknowledgements

Authors gratefully acknowledge the financial support given for this work by the Directorate General of Higher Education, 2015 with contract number: SP DIPA-023.04.1.673453/2015, 14 November 2014, for Kopertis Wilayah X, number: 14/Kontrak/ 010/ KM/ 2015, Indonesia and the Malaysian Ministry of Higher Education (MOHE) under contract number: UKM-GGPM-NBT-078-2010.

## References

- Antar, Z., Feller, J. F., Noël, H., Glouannec, P., & Elleuch, K. (2012). Thermoelectric behaviour of melt processed carbon nanotube/graphite/poly (lactic acid) conductive biopolymer nanocomposites (CPC). *Materials Letters*, 67, 210-214.
- Antunes, R. A., De Oliveira, M. C. L., Ett, G., & Ett, V. (2011). Carbon materials in composite bipolar plates for polymer electrolyte membrane fuel cells: A review of the main challenges to improve electrical performance. *Journal of Power Sources*, 196, 2945-2961.
- Antunes, R. A., Oliveira, M. C. L., Ett, G., & Ett, V. (2010). Corrosion of metal bipolar plates for PEM fuel cells: A review. *International Journal of Hydrogen Energy*, 33, 3632-3647.
- Bin, Y. Z., Matsuo, M., & Zhu, D. (2006). Electrical conducting behaviours in polymeric composites with carbonaceous fillers. *Journal of Polymer Science Part B*, 45, 1037-1044.
- Bodo, F., Florian, H., GojnyMalte, H. G. W., Mathias, C. M. N., & Karl, S. (2006). Fundamental aspects of nano-reinforced composites. *Composite Science Technology*, 66, 3115-3125.
- Cao, M. Y., Rhee, B. O., & Chung, C. I. (1991). Usefulness of the viscosity measurement of feedstock in powder injection molding. *Advances in Powder Metallurgy and particulate materials*, 2, 1991-1995.
- Castro, M., Kumar, B., Feller, J.F., Haddi, Z., Amari, A., & Bouchikhi, B. (2011). Novel e-nose for the discrimination of volatile organic biomarkers with an array of carbon nanotubes (CNT) conductive polymer nanocomposites (CPC) sensors. *Sensor Actuator B-Chemical*, 159, 213-219.
- Chang, E. H., Hong, K. L., Joong, H. L., Nam, H. K., Peng, L., & Yun, K. J. (2009). Effect of carbon fillers on properties of polymer composite bipolar plates of fuel cells. *Journal of Power Sources*, 193, 523-529.
- Chen, C. H., Huang, Y. W., Ma, M. C. C., Su, S. F., Teng, C. C., Weng, C. C., & Yuen, S. M. (2008). Effect of MWCNT content on rheological and dynamic mechanical properties of multiwalled carbon nanotube/ polypropylene composites. *Composite Part A*, 39, 1869-1875.
- Chunhui, S., Mu, P., & Runzhang, Y. (2008). The effect of particle size gradation of conductive fillers on the conductivity and the flexural strength of composite bipolar plate. *International Journal of Hydrogen Energy*, 33, 1035-39.
- Dweiri, R., & Sahari, J. (2007). Electrical properties of carbon-based polypropylene composites for bipolar plates in polymer electrolyte membrane fuel cell (pemfc). *Journal of Power Sources*, 171, 424- 432.
- German, R. M., & Bose. (1997). *Injection molding of metal and ceramic*. Metal Powder Industries Federation. New Jersey, NJ: John Wiley and Sons.
- Ibrahim, M. H. I., Muhamad, N., Sulong, A. B., Jamaluddin, K. R., Ahmad, S., & Nor, N. H. M. (2011). Optimization of micro injection molding with multiple performance characteristic using grey relational grades. *Chiang Mai Journal of Science*, 38, 231-241.
- Ibrahim, M. H. I., Muhamad, N., & Sulong, A. B. (2009). Rheological investigation of water atomized stainless steel powder for micro metal injection molding. *International Journal of Mechanical and Materials Engineering*, 4, 1-8.
- Imai, M., Akiyama, K., Tanaka, T., & Sano, E. (2010). Highly strong and conductive carbon nanotube/cellulose composite paper. *Composite Science Technology*, 70, 1564-1570.
- Kadry, S. 2008. Corrosion Analysis of Stainless Steel. *Journal Science Resources*. 22, 509-516.
- Lee, Y. B., Lee, C. H., Kim, K. M., & Lim, D. S. (2011). Preparation and properties on the graphite/ polypropylene composite bipolar plates with a 304 stainless steel by compression molding for PEM fuel cell. *International Journal of Hydrogen Energy*, 36, 7621-7627.
- Liao, S., Yen, C., Weng, C., Lin, Y., Ma, C., & Yang, C. (2008). Preparation and properties of carbon nanotube/polypropylene nanocomposite bipolar plates for polymer electrolyte membrane fuel cells. *Journal of Power Sources*, 185, 1225-1232.
- Ma, P. C., Siddiqui, N. A., Marom, G., & Kim, J. K. (2010). Dispersion and functionalization of carbon nanotubes for polymer-based nanocomposites: A review. *Composites Part A*, 41, 1345-1367.
- Nishata, R. R. R., Sulung, A. B., Sahari, J., & Suherman, H. (2013). Effect of acid- and ultraviolet/ozonolysis-treated MWCNTs on the electrical and mechanical properties of epoxy nanocomposites as bipolar plate applications. *Journal of Nanomaterials*, 2013, Article ID 717459, 1-8.
- Paul, I. A., Bem, N. G., Justine, N. I., Solaugun, S., & Joy, O. (2012). Evaluation of the corrosion resistance of aluminum alloy matrix 2.5% particulate glass reinforced composite in various media. *International Journal of Science and Technology*, 1, 560-565.
- Rosato, D. V., & Rosato, D. P. E. (1995) *Injection molding hand book: The complete molding operation* (2<sup>nd</sup> Ed.). New York, NY: Chapman and Hall.
- Salamat, M. Z., Sahari, J., Muhamad, N., & Muchtar, A. (2011). The effects of thickness reduction and particle sizes on the properties graphite – Polypropylene composite. *International Journal of Mechanical and Materials Engineering (IJMME)*, 6, 194-200.

- Sharma, M., Rao, I. M., & Bijwe, J. (2009). Influence of orientation of long fibers in carbon fiber-polyetherimide composites on mechanical and tribological properties. *Wear*, 267, 839-845.
- Stobinski, L., Lesiak, B., Kover, L., Toth, J., Biniak, S., & Trykowski, G. (2010). Multiwall carbon nanotubes purification and oxidation by nitric acid studied by the FTIR and electron spectroscopy methods. *Journal of Alloys Compounds*, 501, 77-84.
- Suherman, H., Sulung, A. B., & Sahari, J. (2010). Effect of filler loading concentration, curing temperature and molding pressure on the electrical conductivity of CNTs/graphite/epoxy nanocomposites at high loading of conductive fillers. *International Journal of Mechanical and Materials Engineering*, 5, 74-79.
- Suherman, H., Sulung, A. B., & Sahari, J. (2013). Effect of the compression molding parameters on the in-plane and through-plane conductivity of carbon nanotubes/graphite/epoxy nanocomposites as bipolar plate material for a polymer electrolyte membrane fuel cell. *Ceramic International*, 39, 1227-1284.
- Yang, W. W., Yang, K. Y., & Hon, M. H. (2003). Effects of PEG molecular weights on rheological behavior of alumina injection molding feeds tocks. *Mater Chemical Physics*, 78, 416-424.
- Yimin, L., Liujun, L., & Khalil, K. A. (2007). Effect of powder loading on metal injection molding stainless steels. *Journal of Material Processing and Technology*, 183, 432-439.
- Zhang, R., Dowden, A., Deng, H., Baxendale, M., & Peijs, T. (2009). Conductive network formation in the melt of carbon nanotube/thermoplastic polyurethane composite. *Composite Science and Technology*, 69, 1499-1504.